

Обзор ArXiv/astro-ph,
27 октября – 2 ноября 2023

От Сильченко О.К.

ArXiv: 2311.00025

The Gas Accretion Rate of Galaxies over $z \approx 0 - 1.3$

ADITYA CHOWDHURY,¹ NISSIM KANEKAR,¹ AND JAYARAM N. CHENGALUR¹

¹*National Centre for Radio Astrophysics, Tata Institute of Fundamental Research, Pune, India.*

ABSTRACT

We present here estimates of the average rates of accretion of neutral gas onto main-sequence galaxies and the conversion of atomic gas to molecular gas in these galaxies at two key epochs in galaxy evolution: (i) $z \approx 1.3 - 1.0$, towards the end of the epoch of peak star-formation activity in the Universe, and (ii) $z \approx 1 - 0$, when the star-formation activity declines by an order of magnitude. We determine the net gas accretion rate R_{Acc} and the molecular gas formation rate R_{Mol} by combining the relations between the stellar mass and the atomic gas mass, the molecular gas mass, and the star-formation rate (SFR) at three epochs, $z = 1.3$, $z = 1.0$, and $z = 0$, with the assumption that galaxies evolve continuously on the star-forming main-sequence. We find that, for all galaxies, R_{Acc} is far lower than the average SFR R_{SFR} at $z \approx 1.3 - 1.0$; however, R_{Mol} is similar to R_{SFR} during this interval. Conversely, both R_{Mol} and R_{Acc} are significantly lower than R_{SFR} over the later interval, $z \approx 1 - 0$. We find that massive main-sequence galaxies had already acquired most of their present-day baryonic mass by $z \approx 1.3$. At $z \approx 1.3 - 1.0$, the rapid conversion of the existing atomic gas to molecular gas was sufficient to maintain a high average SFR, despite the low net gas accretion rate. However, at later times, the combination of the lower net gas accretion rate and the lower molecular gas formation rate leads to a decline in the fuel available for star-formation, and results in the observed decrease in the SFR density of the Universe over the last 8 Gyr.

Три масштабировующих соотношения на трех z

- Главная последовательность
- Соотношение $M(\text{HI}) - M_*$
- Соотношение $M(\text{H}_2) - M_*$

Переход к темпам аккреции

$$M_{*,f} = M_{*,i} + \int_{t_i}^{t_f} (1 - f_{return}) \text{SFR}_{\text{MS}}(M_*, t) dt \quad (1)$$

where $\text{SFR}_{\text{MS}}(M_*, t)$ is the main-sequence relation at the time t , and f_{return} is the fraction of the stellar mass returned to the ISM via stellar winds or supernovae ($f_{return} = 0.41$ for a Chabrier IMF; Leitner & Kravtsov 2011; Madau & Dickinson 2014). We define here the average star-formation rate R_{SF} between the epochs t_i and t_f , such that

$$M_{*,f} = M_{*,i} + (1 - f_{return}) R_{\text{SF}} \Delta t \quad (2)$$

where $\Delta t = t_f - t_i$ is the time interval between the two epochs of interest. Measurements of the star-forming main-sequence (e.g. Whitaker et al. 2014; Popesso et al. 2022) can then be used to track the evolution of the stellar mass of a main-sequence galaxy using Equation 1, and this can be combined with Equation 2 to determine R_{SF} using the following relation.

$$R_{\text{SF}} = \frac{(M_{*,f} - M_{*,i})}{(1 - f_{return}) \Delta t} \quad (3)$$

Next, the final molecular gas reservoir¹, $M_{\text{Mol},f}$, of the galaxy at time t_f is related to the initial molecular gas reservoir, $M_{\text{Mol},i}$, at time t_i via

$$M_{\text{Mol},f} = M_{\text{Mol},i} - R_{\text{SF}} \Delta t + R_{\text{Mol}} \Delta t \quad (4)$$

is dissociated to HI. Given that the initial and final stellar masses are known, one can use measurements of the molecular gas mass as a function of stellar mass at both epochs to determine $M_{\text{Mol},f}$ and $M_{\text{Mol},i}$ which can then be combined with Equation 4 to obtain R_{Mol} using the following relation.

$$R_{\text{Mol}} = R_{\text{SF}} + (M_{\text{Mol},f} - M_{\text{Mol},i}) / \Delta t \quad (5)$$

Finally, the neutral atomic gas mass, $M_{\text{Atom},f}$, of the galaxy at time t_f is related to the initial neutral atomic gas mass, $M_{\text{Atom},i}$, at time t_i via the relation

$$M_{\text{Atom},f} = M_{\text{Atom},i} - R_{\text{Mol}} \Delta t + R_{\text{Acc}} \Delta t \quad (6)$$

where R_{Acc} is the *net* accretion rate of neutral atomic gas onto the disk of the galaxy, i.e. the difference between the neutral atomic gas inflow and outflow rates. Again, measurements of M_{HI} as a function of stellar mass at the two epochs can be used to determine $M_{\text{Atom},f}$ and $M_{\text{Atom},i}$, which can be combined with Equation 6 to obtain R_{Acc} using the following relation:

$$R_{\text{Acc}} = R_{\text{Mol}} + (M_{\text{Atom},f} - M_{\text{Atom},i}) / \Delta t \quad (7)$$

We note that in the above formalism, the stellar mass returned to the ISM is assumed to be mostly in the ionised state and is hence not explicitly included in Equations 4-7

Эволюция отдельной галактики

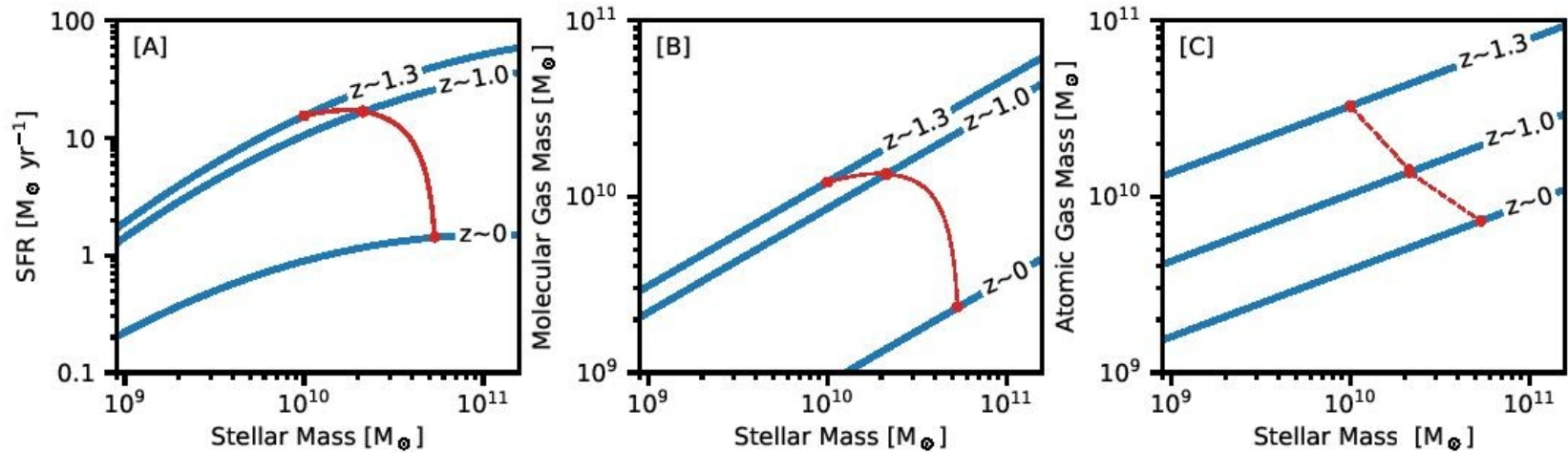


Figure 1. The panels show (in blue), as a function of stellar mass, [A] the SFR (Section 2.2), [B] the molecular gas mass (Section 2.3), and [C] the atomic gas mass (Section 2.4), for main-sequence galaxies at $z \approx 0$, $z \approx 1.0$ and $z \approx 1.3$. The red curve in Panel [A] shows the evolutionary track of a galaxy with $M_* = 10^{10} M_\odot$ at $z \approx 1.3$, obtained using Equation 1. The corresponding evolution of the molecular gas mass, obtained using Equations 1 and 9, is shown in Panel [B]. Finally, the red points in Panel [C] shows the atomic gas mass of the galaxy at the three redshifts, obtained using Equation 14. Note that the $M_{\text{Atom}} - M_*$ relation of Equation 14 is not a continuous function of redshift; the dashed line in the panel is hence only for visual aid, showing a linear interpolation between the points. See main text for discussion.

Эволюция темпов аккреции

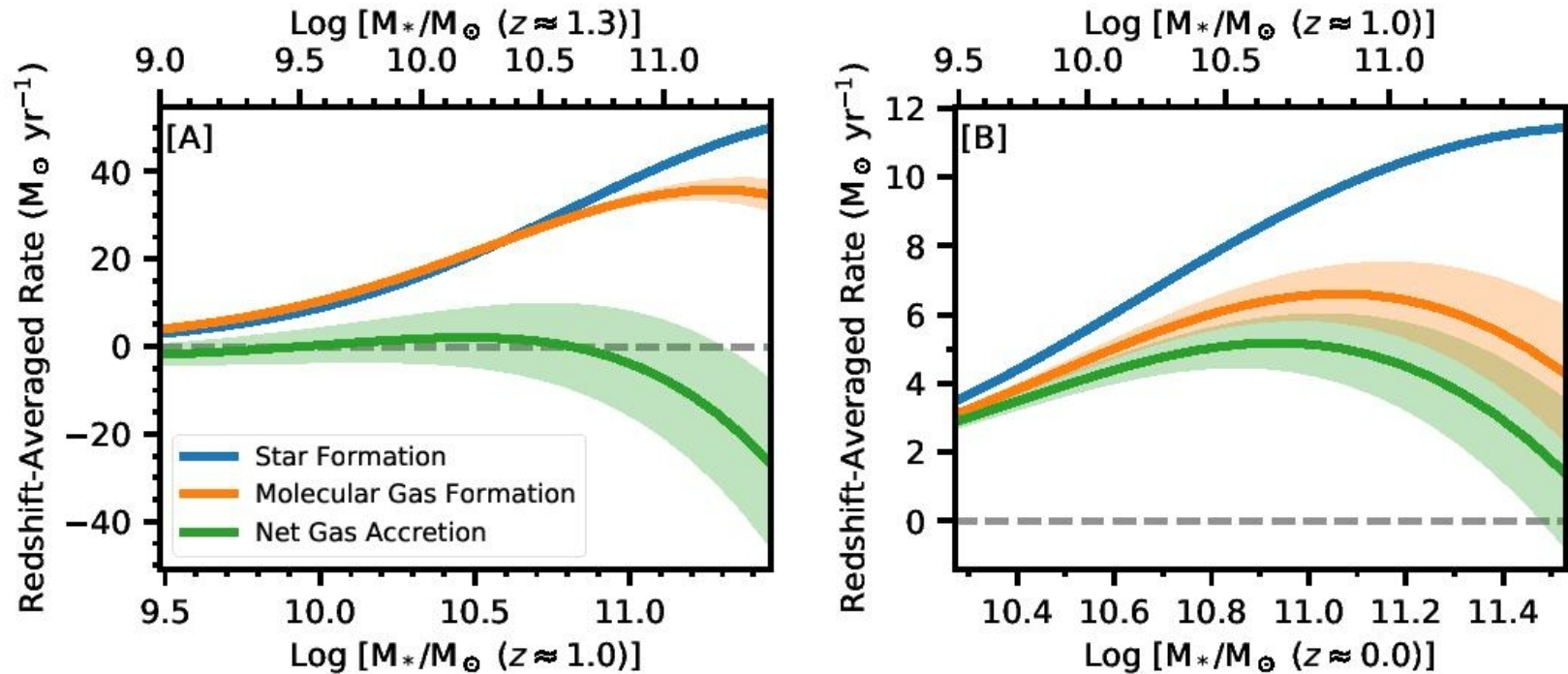


Figure 2. The two panels show the redshift-averaged star-formation rate (R_{SF} , in blue), molecular gas formation rate (R_{Mol} , in orange), and net gas accretion rate (R_{Acc} , in green) of main-sequence galaxies, as a function of the stellar mass, over [A] $z = 1.3$ to $z = 1.0$, and [B] $z = 1.0$ to $z = 0$. The shaded regions around each curve show the 68% confidence intervals. The top x-axis of panel [A] shows the initial stellar mass of the galaxies at $z = 1.3$, while the bottom x-axis shows the final stellar mass, at $z = 1.0$. This final stellar mass at $z = 1.0$ is plotted as the top x-axis of panel [B], with the bottom axis of the panel showing the final stellar mass of the galaxies at $z = 0$. The evolution of the stellar masses was obtained using Equation 1. Panel [A] shows that the molecular gas formation rate and star-formation rates are similar for all but the most massive galaxies over the interval $z = 1.3$ to $z = 1.0$, but the net gas accretion rate over the same period is much lower than the other two rates. Panel [B] shows that both the average molecular gas formation rate and the average net gas accretion rate are lower than the average SFR for the lower-redshift interval, $z = 1.0$ to $z = 0$, for galaxies of all stellar masses. See main text for discussion.

Эволюция барионной массы

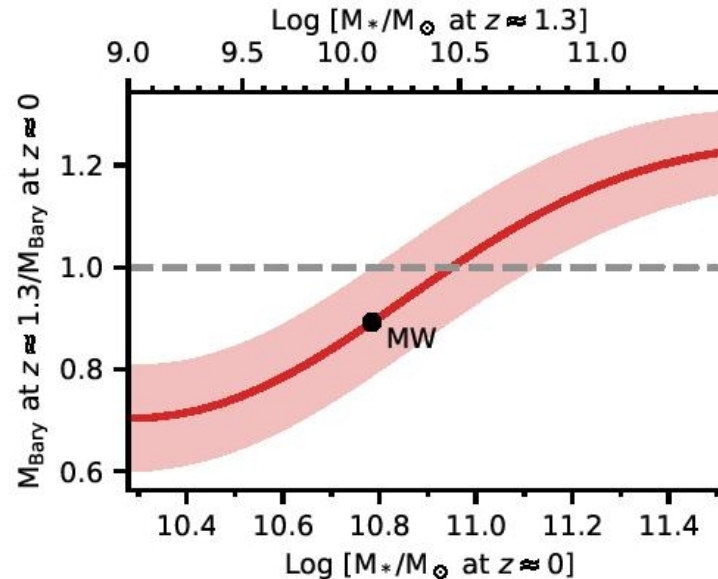


Figure 3. The ratio of the baryonic mass of main-sequence galaxies at $z \approx 1.3$ to that at $z = 0$, as a function of their stellar mass at $z \approx 0$. The black dot indicates the position on the relation of a galaxy with the stellar mass of the Milky Way today. The dashed horizontal line is at a ratio of 1, indicating no change in the baryonic mass between $z = 1.3$ and $z = 0$. It is clear that the highest-mass ($M_* \gtrsim 10^{10.5} M_\odot$ at $z \approx 1.3$) galaxies had the bulk of their baryonic mass in place by $z \approx 1.3$; the baryonic mass of these galaxies has declined over the past ≈ 9 Gyr. Conversely, the baryonic mass of galaxies with stellar mass $M_* \lesssim 10^{10} M_\odot$ at $z \approx 1.3$ has increased since $z \approx 1.3$, by approximately 30% for galaxies with $M_* \approx 10^9 M_\odot$ at $z \approx 1.3$.